Biochemical Pharmacology xxx (xxxx) xxx–xxx

Contents lists available at ScienceDirect

Biochemical Pharmacology

journal homepage: www.elsevier.com/locate/biochempharm

EHP-101, an oral formulation of the cannabidiol aminoquinone VCE-004.8, alleviates bleomycin-induced skin and lung fibrosis

Adela García-Martín[a], Martín Garrido-Rodríguez[b], Carmen Navarrete[a], Carmen del Río[c,d,e], María L. Bellido[a,f], Giovanni Appendino[g], Marco A. Calzado[c,d,e], Eduardo Muñoz[c,d,e,*]

[a] Vivacell Biotechnology España, Córdoba, Spain
[b] Innohealth Group, Madrid, Spain
[c] Instituto Maimónides de Investigación Biomédica de Córdoba (IMIBIC), Córdoba, Spain
[d] Departamento de Biología Celular, Fisiología e Inmunología, Universidad de Córdoba, Córdoba, Spain
[e] Hospital Universitario Reina Sofía, Córdoba, Spain
[f] Emerald Health Pharmaceuticals, San Diego, USA
[g] Dipartimento di Scienze del Farmaco, Università del Piemonte Orientale, Novara, Italy

ARTICLE INFO

Keywords:
Cannabinoids
Systemic fibrosis
Bleomycin
Inflammation
Transcriptomic signature

ABSTRACT

Systemic sclerosis (SSc) or scleroderma is a chronic multi-organ autoimmune disease characterized by vascular, immunological, and fibrotic abnormalities. The etiology of SSc is unknown, but there is growing evidence that dysfunction of the endocannabinoid system (ECS) plays a critical role in its development. Since the semi-synthetic cannabinoquinoid VCE-004.8 could alleviate bleomycin (BLM)-induced skin fibrosis, we have investigated an oral lipid formulation (EHP-101) of this dual PPARγ/CB_2 receptors activator for the prevention of skin- and lung fibrosis and of collagen accumulation in BLM challenged mice. Immunohistochemistry analysis of the skin showed that EHP-101 could prevent macrophage infiltration as well as the expression of Tenascin C (TNC), vascular cell adhesion molecule 1 (VCAM1), and the α-smooth muscle actin (SMA). EHP-101 could also prevent the reduced expression of vascular CD31 typical of skin fibrosis. RNAseq analysis of skin biopsies showed a clear effect of EHP-101 in the inflammatory and epithelial-mesenchymal transition transcriptomic signatures. TGF-β-regulated genes [matrix metalloproteinase-3 (Mmp3), cytochrome b-245 heavy chain (Cybb), lymphocyte antigen 6E (Ly6e), vascular cell adhesion molecule-1 (Vcam1) and Integrin alpha-5 (Itga5)] were induced in BLM mice and repressed by EHP-101 treatment. By intersecting differentially expressed genes in EHP-101-treated mice with a dataset of human scleroderma intrinsic genes, 53 overlapped genes were discovered, including biomarkers of SSc like the C-C motif chemokine 2 (Ccl2) and the interleukin 13 receptor subunit alpha 1 (IL-13Ra1) genes. Taken together, these data provide a rationale for further developing VCE-004.8 as an orally active agent to alleviate scleroderma and, possibly, other fibrotic diseases as well.

1. Introduction

Systemic sclerosis (SSc) or scleroderma is a chronic multiorgan autoimmune disease of unknown etiology characterized by immunological, vascular, and fibrotic abnormalities. The disease is complex and dynamic, and the interrelationship among the main hallmarks of SSc results in a wide spectrum of clinical presentations ranging from limited skin involvement (limited cutaneous SSc; lSSc) to widespread internal organ fibrosis (diffuse cutaneous SSc; dSSc). Independently to the clinical subtypes, several studies have highlighted the importance to identify different gene expression profiles within scleroderma patients in order to provide a more personalized diagnosis and/or treatment [1,2]. Accordingly, a study analyzing the transcriptome in skin biopsies from 27 scleroderma patients has defined two subtypes of the disease at

Abbreviations: AjA, Ajulemic Acid; BLM, Bleomycin; CBD, Cannabidiol; Ccl2, C-C motif chemokine 2; Cybb, cytochrome b-254 heavy chain; dSSc, diffuse cutaneous systemic sclerosis; ECS, Endocannabinoid system; ly6e, IL-13Ra1, Interleukin 13 receptor subunit alpha1; Itga5, Integrin alpha-5 lymphocyte antigen 6E; lSSc, limited cutaneous systemic sclerosis; Mmp3, matrix metalloproteinase-3; RGZ, Rosiglitazone; SMA, α-smooth muscle actin; SSc, Systemic sclerosis; Col7a1, Type VII collagen; TNC, Tenascin C; VCAM1, vascular cell adhesion molecule 1 protein; VIM, Vimentin

* Corresponding author at: Instituto Maimónides de Investigación Biomédica de Córdoba, Universidad de Córdoba, Avda Menéndez Pidal s/n. 14004, Córdoba, Spain.
E-mail address: fi1muble@uco.es (E. Muñoz).

https://doi.org/10.1016/j.bcp.2018.07.047
Received 9 June 2018; Accepted 31 July 2018

the transcriptomic level. Namely, a fibroproliferative signature type that predominate in patients with dSSc subclinical type, and an inflammatory signature type, which was detected preferentially in dSSc, lSSc and Morphea patients [3].

The endocannabinoid system (ECS) is composed by the GPRC receptors CB_1 and CB_2, the endocannabinoids, mainly anandamide and 2-arachidonoyl glycerol, and the enzymes that regulated their synthesis and catabolism. In addition, some endogenous and exogenous cannabinoids also target ionotropic receptors of the TRP family, non-canonical GPR receptors such as GPR55, and nuclear receptors such as PPARα and PPARγ, adding additional complexity to the functionality of the ECS [4,5].

There is growing evidence that the ECS could play a role in the pathophysiology of SSc. Thus, it has been shown that CB_1 and CB_2 receptors are expressed in SSc fibroblasts [6], and the anti-inflammatory and anti-fibrotic actions of cannabinoids have been clearly demonstrated in different experimental models. For instance, genetic inactivation of CB_1 receptor reduces fibrosis in experimental models of SSc indirectly through the inhibition of leukocyte infiltration in the damaged tissue [7]. Accordingly, pharmacological activation of CB_1 receptor exacerbates fibrosis induced by bleomycin (BLM) [7]. Conversely, CB_2 receptor plays a protective role against fibrosis and reduces inflammatory infiltrates in experimental models of SSc [8,9]. Indeed, inhibition of CB_2 receptor increase the susceptibility to develop fibrosis in live [8].

PPARγ was initially identified because of its role in the regulation of glucose and lipid metabolism, but PPARγ ligand agonists are also endowed with anti-inflammatory and anti-fibrotic activities [10,11]. In this context, PPARγ is a regulator of connective tissue homeostasis, and different experimental approaches have shown that PPARγ ligands attenuate hepatic- [12] renal- [13], and pulmonary fibrosis [14] as well as BLM-induced skin fibrosis [15–18]. Thus, structurally different CB_2 agonists such as JHW-133, and dual PPARγ/CB_2 agonists such as Ajulemic acid (AjA) and VCE-004.8 have been shown to alleviate skin fibrosis and inflammation in experimental models of SSc [19,15,16]. Moreover, AjA (Lenabasum) has shown efficacy in a Phase 2 clinical trial with dSSc patients (clinicaltrial.gov identifier: NCT02465437), while a recent study suggested that AjA ameliorates inflammation through the generation of pro-resolvin lipid mediators in human volunteers [20]. The relative contribution of CB_2 receptor, PPARγ or of both pathways to this activity is still unclear.

We have shown previously that VCE-004.8 is a multitarget CBD derivative acting as a dual PPARγ/CB_2 agonist and as an activator of the HIF pathway [16,21]. VCE-004.8 [(1′R,6′R)-3-(Benzylamine)-6-hydroxy-3′-methyl-4-pentyl-6′-(prop-1-en-2-yl) [1,1′bi(cyclohexane)]-2′,3,6-triene-2,5-dione)] has been granted Orphan Drug designation by the FDA and EMA for Systemic Scleroderma. We now report that EHP-101, an oral lipidic formulation of VCE-004.8, prevents skin and lung fibrosis in a BLM-model of SSc. By transcriptomic analyses, we also demonstrate that EHP-101 downregulates the expression of several key genes associated with fibrosis and inflammation. Taken together, these results provide a rationale for further developing VCE-004.8 as a treatment of scleroderma and, possibly, other fibrotic diseases as well.

2. Material and methods

2.1. Animals and experimental protocols

Six- to eight-week-old female BALB/c mice were purchased from Harlan laboratories (Barcelona, Spain) and housed in our animal facilities (University of Córdoba, Córdoba, Spain) under controlled conditions (12 h light/dark cycle; temperature 20 °C (± 2 °C) and 40–50% relative humidity) with free access to standard food and water. All experiments were performed in accordance with European Union guideline and approved by the Animal Research Ethic Committee of the Córdoba University (2014PI/016).

Dermal fibrosis was induced by daily subcutaneous injections of filter-sterilized bleomycin (20 µg/mouse diluted in PBS) (Mylan Pharmaceuticals, Barcelona, Spain) into the shaved backs well-defined areas (1 cm^2) of mice for 6 weeks. During the last 3 weeks of bleomycin injections, mice were treated daily by oral gavage with different concentrations of EHP-101 (5, 10 and 25 mg/kg) or vehicle alone. EHP-101 is a formulated solution of VCE-004.8 (30 mg/ml) dissolved in lipid solvent. In parallel mice were injected intraperitoneally (ip) with RGZ (5 mg/kg) (Cayman Chemical, Ann Arbor, MI, USA). At the end of the experimental procedure, mice were sacrificed and dissected for tissue processing. Skin and lung samples were frozen in RNA-later (Sigma-Aldrich, St. Louis, MO, USA) cooled in dry ice and stored at −80 °C for transcriptomic analysis or fixed in fresh 4% paraformaldehyde (0.1M, PBS) (AppliChem, Darmstadt, Germany) for histochemical analysis. Ten to six animals were analyzed in each experimental group.

2.2. Histochemical analysis

Skin or lung sections (5 µm-thick) were stained with Masson's trichrome (Merck Millipore, Darmstadt, Germany). Skin collagen was detected by picrosirius red staining (Sigma-Aldrich, St. Louis, MO, USA). For immunohistochemical detection of macrophages, we used F4/80 (1:50, #MCA497, Bio Rad Laboratories, Hercules, CA, USA) antibody. Slides were developed with diaminobenzidine chromogen (Merck, Darmstadt, Germany) and counterstained in Harris haematoxylin (AppliChem, Darmstadt, Germany). Three random fields of each skin or lung biopsy were photographed, digitalized using a Leica DFC420c camera and analyzed using Image J software in a blinded manner by two independent observers. The Ashcroft score was used to determine the degree of fibrosis in lung specimens as previously described [22,23].

2.3. Confocal analyses

For antigen retrieval, paraffin-embedded skin section (5 µm-thick) were deparaffinized and boiled for 10 min in sodium citrate buffer (10 mM, pH 6.0) (Sigma-Aldrich, St. Louis, MO, USA). The sections were washed three times in PBS. Nonspecific antibody-binding sites were blocked for 1 h at room temperature with 3% bovine serum albumin (BSA) (Sigma-Aldrich, St. Louis, MO, USA in PBS). Next, the sections were incubated overnight at 4 °C in following primary antibodies diluted in PBS with 3% BSA: rabbit polyclonal anti-CD31 (1:100 dilution, ab28364, Abcam, Cambridge, UK), rabbit monoclonal anti-VCAM1 (1:100 dilution, ab134047, Abcam, Cambridge, UK), monoclonal rat anti-Tenascin (TNC) (1:100 dilution, #MAB2138, RD system, Mineapolis, MN, USA), mouse anti-Vimentin (VIM) (1:100 dilution, #550513, BD biosciences, San Jose, CA USA) and α-Smooth muscle actin (SMA) monoclonal antibody Alexa-488 (1:100 dilution, #53-9760-80, Thermo Fischer, Walthamm, MA, USA). After extensive washing in PBS, slides were incubated with secondary antibodies for 1 h at room temperature in the dark. The inmunoreactions were revealed using anti-rabbit Texas Red (1:100 dilution, #A-6399), anti- rat Alexa 488 (1:100 dilution, #A-11006), anti-mouse Alexa 647 (1:100 dilution, #A-21235) were obtained by Thermo Fischer Scientific, Walthamm, MA, USA. The tissue sections were then mounted Vectashield Antifade Mounting Medium with DAPI (H-1200, Vector Laboratories, Burlingame, Ca, USA). All images were acquired using a spectral confocal laser-scanning microscope LSM710, (Zeiss, Jena, Germany) with a 25×/0.8 Plan-Apochromat oil immersion lens and quantified in 10–15 randomly chosen fields using ImageJ software (http://rsb.info.nih.gov/.ij).

2.4. RNA sequencing

Total RNA was isolated from mice frozen skin tissue using QIAzol lysis reagent (Qiagen, Hilden, Germany) and purified with RNeasy mini

kit (Qiagen, Hilden, Germany). Transcriptome libraries were constructed with TruSeq Stranded Total RNA LT Sample Prep Kit (with Ribo-Zero Human/Mouse/Rat, #RS-122-2201, Illumina, San Diego, USA). In brief, 300 ng of total RNA from each sample was used to construct a cDNA library, followed by sequencing on the Illumina Hiseq 2500 with single end 50 bp reads and ~30 millions of reads per sample.

2.5. Bioinformatics and data analysis

Sequencing data have been uploaded in the Gene Expression Omnibus (GEO) database and can be viewed with the accession number of GSE115503. The sequences were pre-processed with Trimmomatic version 0.36 [24] and aligned to mouse genome assembly mm10 using HISAT2 version 2.1.0 [25]. Counts per gene were obtained with feature Counts version 1.6.1 [26] using the in-built Ref Seq annotation for mm10 genome assembly. The raw counts were then analyzed with DESeq2 version 1.20.0 [27] excluding those genes with less than 10 counts across all samples, resulting in a total of 18,985 genes. The differential expression analysis was performed using the negative binomial linear models included in DESeq2. All genes with an adjusted p value < 0.05 were considered as differentially expressed genes (DEGs). Cluster Profiler version 3.8.9 [28] and the annotation package org.Mm.eg.db version 3.5.0 were employed to identify overrepresented Gene Ontology (Biological Process) terms in the sets of genes after splitting them into up and down regulated DEGs. For a term to be considered as enriched in any group of DEGs, it must contain at least 10 genes and present an enrichment adjusted p value < 0.05. The MSigDb hallmarks version 6.1 [29] "Inflammatory Response" and "Epithelial Mesenchymal Transition" were intersected with the DEGs upregulated by bleomycin and downregulated by EHP-101 to create the transcriptomic signatures. To obtain the intersection with the human scleroderma intrinsic genes, we collapsed the list of intrinsic genes included in the GEO dataset GSE9285 with the list of common DEGs in our comparisons. The HUGO gene symbol nomenclature was used to intersect our data with human genes.

2.6. Statistical analysis

All the *in vivo* data are expressed as the mean ± SEM. Unpaired two-tailed student T test for parametric analysis of two samples or Kruskal-Wallis test were used to determine the statistical significance in the case of non-parametric analysis. The level of significance was set at $p < 0.05$. Statistical analyses were performed using GraphPad Prism version 6.00 (GraphPad, San Diego, CA, USA).

3. Results

3.1. Effect of formulated VCE-004.8 (EHP-101) on skin and lung fibrosis

VCE-004.8 is a multitarget compound showing *in vivo* anti-fibrotic and anti-inflammatory activity after intraperitoneal administration [16,21]. To study the activity after oral administration, VCE-004.8 was formulated in a lipidic matrix (EHP-101), and its effectiveness was evaluated in a murine model of SSc. Skin fibrosis was induced according to a previously established protocol [30], and no sign of toxicity was observed during the experimental procedure. In BLM-challenged mice, a significant increase of dermal thickness and collagen contents was observed, paralleled by a reduction of subcutaneous adipose layer that was replaced by connective tissue. Oral EHP-101 (5, 10, 25 mg/kg) alleviated skin fibrosis, reducing skin thickness to levels similar to those of RGZ (5 mg/kg) that served as a positive control for PPARγ activation. In addition, higher doses of EHP-101 were also capable of recovering lipoatrophy (Fig. 1A and B) [31].

Excessive collagen deposition is a key marker of BLM-induced skin fibrosis [32]. To evaluate this parameter, dermal expression of collagen was assessed by quantification of picrosirius red staining of skin. As depicted in Fig. 1C, an increase in collagen accumulation was observed in BLM mice compared to control animals, and treatment with EHP-101 prevented this accumulation. It has been previously shown that BLM-induced fibrosis is associated with macrophage infiltration and activation, [33,16]. Thus, we evaluated the effect of EHP-101 treatment on the recruitment of inflammatory cells by measuring the infiltration of F4/80(+) macrophages in the skin of BLM-challenged mice. We found that EHP-101, as well as RGZ, inhibited macrophage infiltration induced by BLM (Fig. 1D).

Next, we evaluated if BLM injection at the skin level could also promote fibrosis in other organs such as lungs. This was the case, but both BLM-induced lung fibrosis (Ascroft scores) and collagen deposition (picrosirius red staining) were alleviated by the treatment with EHP-101 (Fig. 2A and B).

3.2. EHP-101 prevents perivascular collagen accumulation and maintains vascular integrity

Vascular damage is a fundamental part of the pathogenesis of scleroderma since the early stages of the disease [34,35]. BLM has been reported to significantly increase the thickness of vascular wall, mimicking some of histologic features found in human SSc [31]. As depicted in Fig. 3A, BLM induced a significant collagen deposition around blood vessels that could, however, be prevented by EHP-101 (25 mg/kg) (Fig. 3A). In addition, a morphometric analysis was performed by measuring blood vessels perimeter with CD31 as an endothelial marker. Remarkably, the average vessel perimeters were significantly decreased in BLM untreated mice compared to control mice group, and it was recovered in EHP-101 treated mice (Fig. 3B and C).

Aberrant proliferation of smooth muscle cells and myofibroblast differentiation is one of the most important elements of the proliferative vasculopathy associated to SSc [34,36]. In the skin of control mice, α-SMA expression was mostly restricted to vascular muscle cells surrounding the vessels (Fig. 3B), increased by BLM treatment and prevented by the administration of EHP-101 (Fig. 3B and C). Finally, we also analyzed the expression of TNC, another relevant marker of fibrosis [37], whose expression was low in control mice, but increased in the skin of BLM mice and could be normalized by EHP-101 treatment (Fig. 3B and C).

3.3. EHP-101 restores normal skin phenotype at transcriptomic level

To study the transcriptomic changes produced by the treatment at tissue level, an RNA-Seq analysis was performed in the skin of the different experimental groups. A differential expression analysis between the various groups identified a total of 4086 genes with an adjusted p value < 0.05 when comparing the BLM group with the control, and 1959 when comparing EHP-101 treated BLM mice vs. untreated BLM (Fig. 4A). To characterize those changes at the biological level, a functional analysis using the Gene Ontology (Biological Process) annotation was carried out. Fig. 4B shows selected enriched terms across the subgroups of differentially expressed genes (DEGs).

Terms associated with the pathogenesis of the disease and enriched in the genes upregulated by BLM and downregulated by EHP-101 can be classified as "positive regulation of cytokine production", "angiogenesis", "interleukin-6 production", "response to interferon-gamma", "response to wounding" and "response to transforming growth factor", in accordance with the dysregulation of the autoimmune, vascular and fibrotic processes [2], and with our previous study that demonstrated the beneficial effects of VCE-004.8 (Figs. 1–3).

Next, to further investigate the effects of the EHP-101 treatment at the transcriptomic level and related to inflammatory and fibrotic processes, we intersected the genes contained in the MSigDb hallmarks [29] "Inflammatory Response" and "Epithelial Mesenchymal Transition" with DEGs upregulated by BLM that were inhibited by EHP-101 (Fig. 4C), finding two transcriptomic signatures of repression in

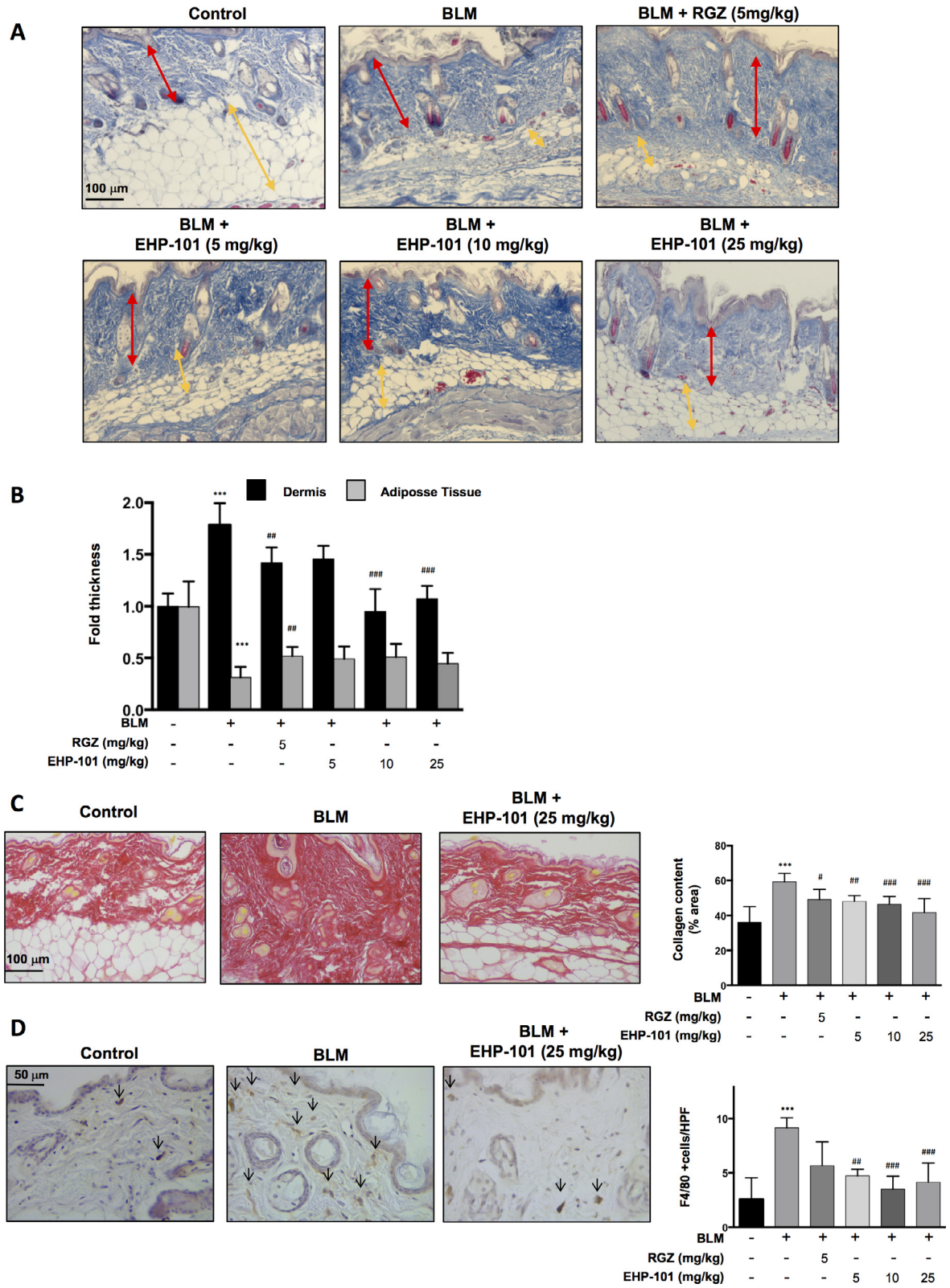

Fig. 1. EHP-101 reduces dermal thickening, collagen accumulation and macrophage infiltration induced by BLM on fibrotic skin. (A) Images show Massońs trichrome staining and (B) their respective quantification of skin from BLM-treated mice. (C) Representative images of collagen staining by picrosirius red dye (left panel) and their quantification (right panel). (D) Images show immunostaining of skin sections for the macrophage specific marker F4/80 (indicated with arrows) (left panel). Quantification of F4/80(+) cells in skin (right panel). Values are expressed as mean ± SEM (n = 8 animals per group). ***p < 0.001 versus control group; # p < 0.05, ##p < 0.01, ###p < 0.001 versus BLM group.

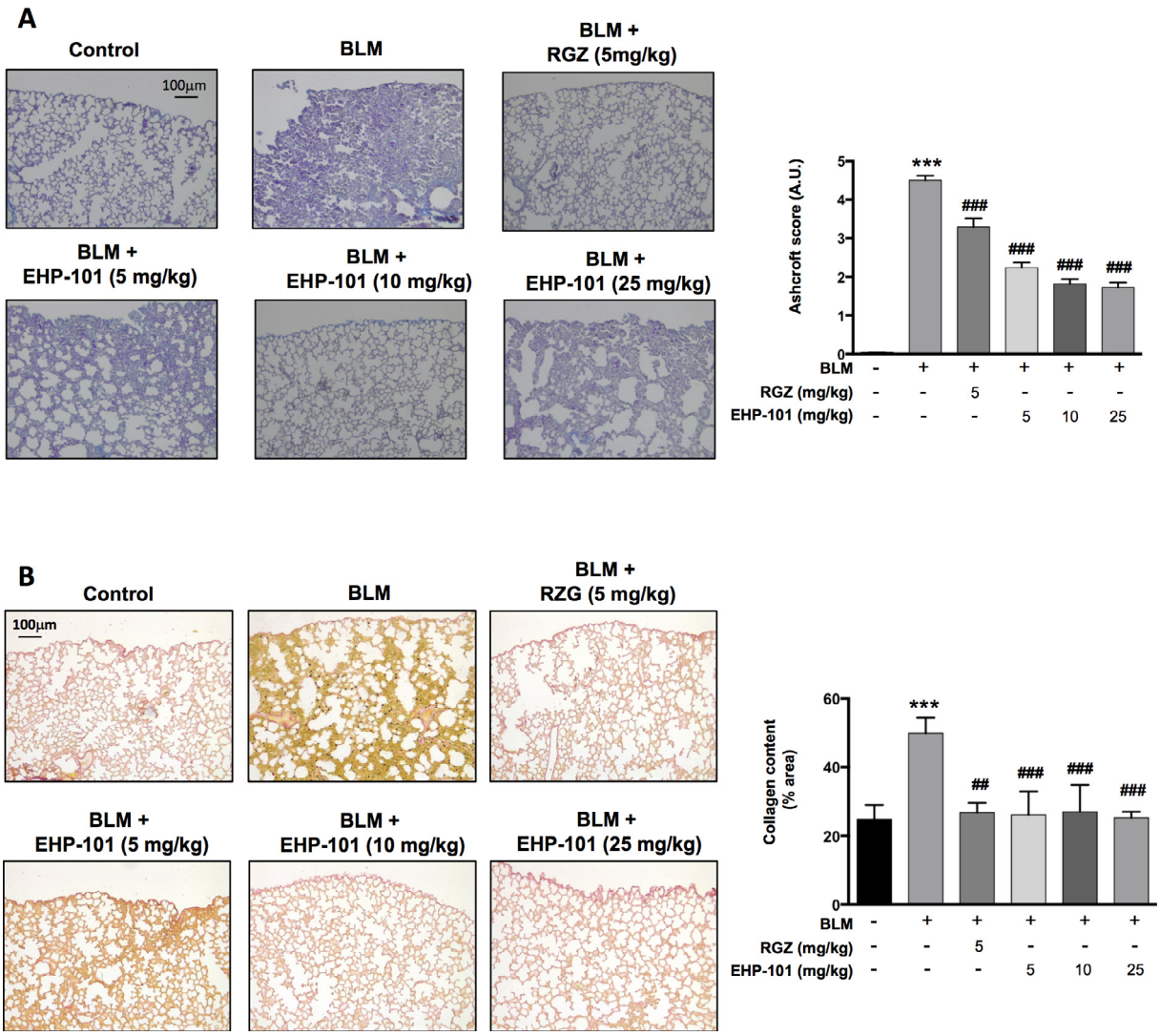

Fig. 2. EHP-101 prevents lungs fibrosis. (A) Representative lungs images of Masson's trichrome staining (left panel). Comparison of the Ashcroft score among the experimental groups (right panel). (B) Representative images of collagen staining by picrosirius red dye and (left panel) their quantification (right panel). Values are expressed as mean ± SEM (n = 8 animals per group). ***p < 0.001 versus control group; ##p < 0.01, ###p < 0.001 versus BLM group.

different genes from those hallmarks. Finally, to evaluate the translation potential of these results, we intersected DEGs in both comparisons with a dataset of human scleroderma "intrinsic" genes obtained from a previous study [3]. From the list of 995 genes, 52 overlapped with genes that change differentially with BLM and EHP-101 treatment (Fig. 4D). To validate the transcriptomic analysis to some extent we studied the expression of VCAM1 and Vimentin (VIM) at the protein level. As depicted in Fig. 5, an increase of VCAM1 and VIM expression was observed in the lesioned skin of BLM mice compared to the control group, which was prevented by EHP-101 treatment. Taken together, these results suggest that the EHP-101 can restore the normal status of mice skin at transcriptomic level through the down regulation of several key genes implicated in the inflammatory fibrotic process.

4. Discussion

Several epidemiology studies have been conducted worldwide in the past 20 years and although there is some variability in the reported estimates in different studies and countries, the prevalence is estimated at around 1–9/100,000 for localized scleroderma, and 1/6500 adults for systemic sclerosis, being females more affected than males (ratio around 4:1). Despite recent progress in the understanding of SSc pathophysiology, the current therapeutic recommendations are concerned with the management of organ specific morbidity and no single therapeutic agent has been proven to be efficacious as a universal disease-modifying agent, that provides benefit to SSc patients regardless of which organs are affected by the disease [38].

We have shown previously that VCE-004.8 is a multitarget CBD derivative acting as a dual PPARγ/CB_2 agonist and as an activator of the HIF pathway [16,21], and herein we report that EHP-101, an oral lipidic formulation of VCE-004.8, could prevent skin and lung fibrosis in a bleomycin-model of SSc.

Several lines of evidence strongly suggest that blocking TGFβ signaling represents a therapeutic approach in fibrosis. In this sense, ligand-activated PPARγ competes for the interaction of p300 to SMAD proteins and inhibits SMAD/p300 complex formation, which is required for TGFβ-induced collagen gene transcription [39]. Thus, CB_2 agonists are able to inhibit VCAM1 expression in endothelial cells acting partially through the PPARγ pathway [40]. Other reports have shown that PPARγ activation can selectively inhibit the induction of VCAM1 [41–43]. On the other hand, CB_2 receptor activation may also be involved in the anti-inflammatory activity of VCE-004.8, possibly by inhibition the production of pro-inflammatory cytokines such as IL-1β and IL-6 in macrophages. Accordingly, CB_2 receptor activation is

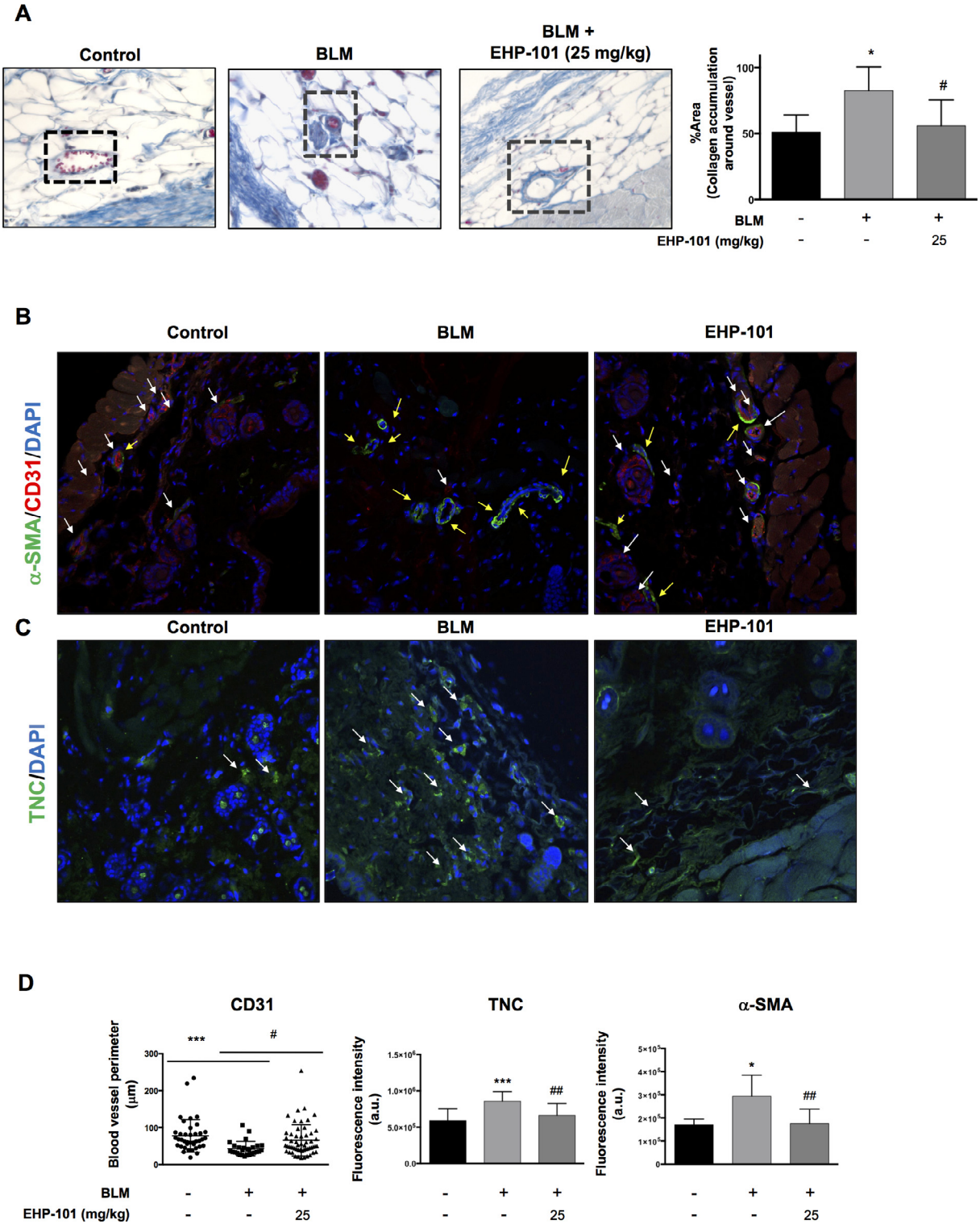

Fig. 3. EHP-101 prevents skin fibrosis. (A) EHP-101 prevents BLM-induced collagen accumulation around blood vessels. Representative images of Masson's trichrome stained skin sections showing collagen associated to blood vessels (indicated with frames) (left panel). Quantification of collagen accumulation in skin (right panel). (B) Double immunoflurescence labelling of skin (CD31, red fluorescence) and smooth muscle cells (α-SMA, green fluorescence) in control, BLM + vehicle and BLM + EHP-101 are shown. CD31 vessels are marked by white arrows, and α-SMA cells are marked by yellow arrows. (C) Immunoflurescence labelling of TNC (green fluorescence) in control, BLM + vehicle and BLM + EHP-101 is shown (original magnification × 25). (D) Quantification of CD31 vessel staining (average vessel perimeter), and expression of TNC and α-SMA. Values are expressed as mean ± SEM (n = 8 animals per group). **p < 0.01, *p < 0.05 versus control group, ##p < 0.01 versus BLM group.

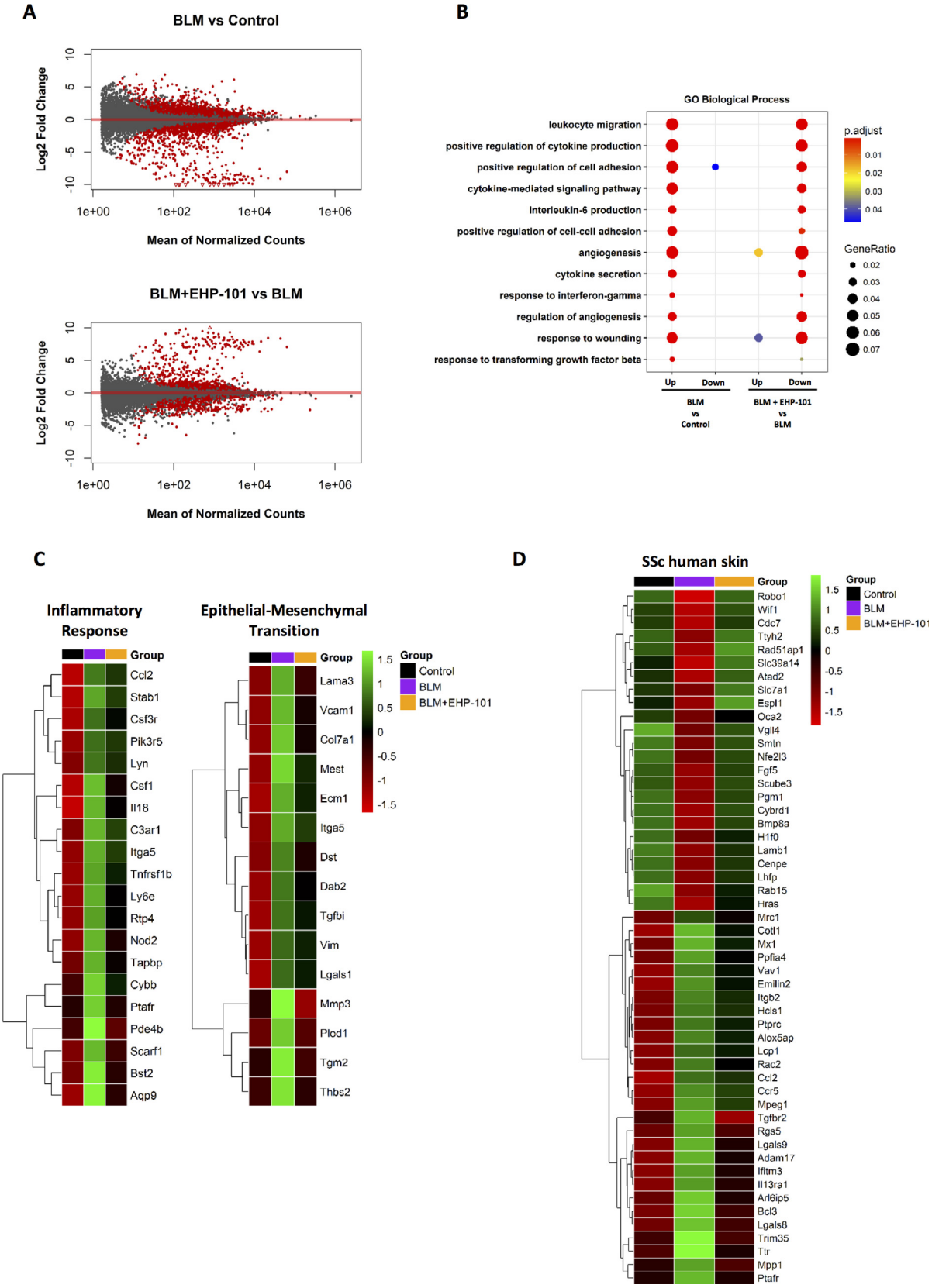

Fig. 4. Gene expression profiling of the effect of EHP-101 in skin. (A) MA plots of the result for the differential expression analyses. Red points represent the differentially expressed genes (adjusted $p < 0.05$). (B) ClusterProfiler results. The dotplot represent the enrichment of selected terms over the different groups. The presence of a point indicates a significant enrichment of a term in a group of genes (adjusted $p < 0.05$). (C) Heatmaps showing the expression levels of genes that increase their expression with the bleomycin treatment and reduce it with EHP-101 inside the selected MSigDb hallmarks (adjusted $p < 0.05$). (D) Heatmap showing the expression levels of 52 genes that are differentially expressed in both comparisons (adjusted $p < 0.05$) and overlap with the group of intrinsic human scleroderma skin expressed genes. The color represents the mean of scaled regularized log transformed expression values.

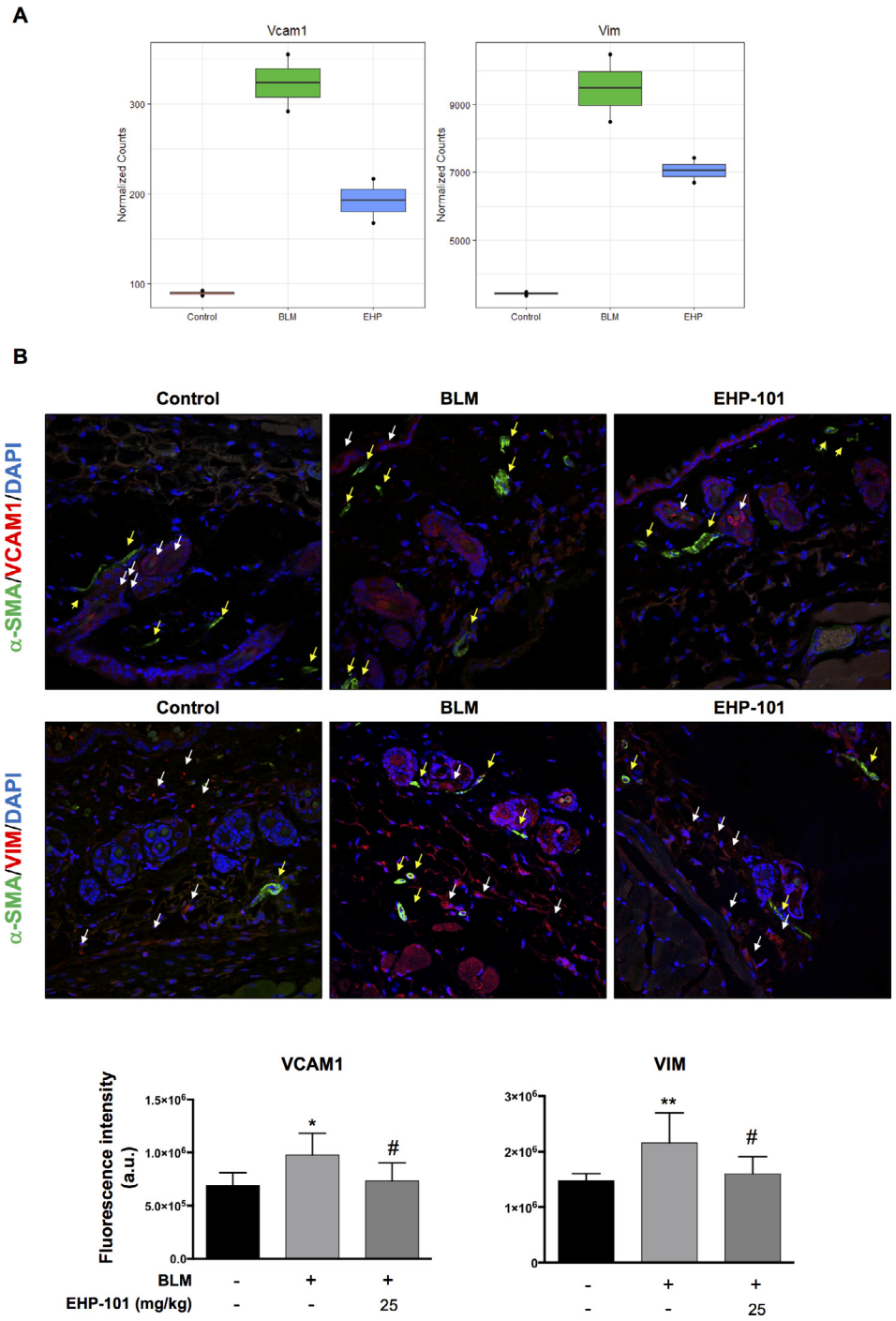

Fig. 5. Effect of EHP-101 on VCAM-1 and VIM expression in the skin (A) Boxplot of DESeq2 normalized counts indicating the detected expression level of Vcam1 and Vim through RNA-Seq. (B) Double immunoflurescence labelling of skin (VCAM-1, red fluorescence) (VIM, red fluorescence) and smooth muscle cells (α-SMA, green fluorescence) in control, BLM + vehicle and BLM + EHP-101 are shown. VCAM-1 and VIM fluorescence are marked by white arrows and α-SMA cells are marked by yellow arrows (top panel). The quantification of expression of VCAM-1 and VIM (bottom panel). Values are expressed as mean ± SEM (n = 8 animals per group). **p < 0.01, *p < 0.05 versus control group; #p < 0.05 versus BLM group.

considered beneficial in fibrotic diseases, and JWH-133, a CB_2 selective agonist, has been shown to decrease the inflammatory infiltrate in the liver of fibrotic animals [44]. Additional evidence has been reported that CB_2 receptor activation inhibits dermal fibrosis by preventing leukocyte infiltration and the release of profibrotic mediators [8]. Taken together, these considerations suggest that EHP-101 prevents BLM-induced skin fibrosis and inflammation and this effect it is likely to be mediated by targeting both PPARγ and CB_2 pathways as described previously for VCE-004.8 [16].

We also found that EHP-101 attenuated levels of TNC in the skin of BLM mice. TNC contributes to the pathogenesis of SSc by eliciting the response of endogenous activator of Toll-like receptor 4 (TLR4) [36,45]. Interestingly, in some disease models, PPARγ agonists have been shown to exert anti-inflammatory effects through suppression of the expression and activity of TLR4 [46,47]. Consistent with this, EHP-101 might attenuate the expression of TNC by inhibiting TLR4 activation through PPARγ activation. Moreover, it has been shown that both IL-4 and IL-13 upregulates TNC synthesis [48,49]. Indeed, we have described that VCE-004.8 (i.p.) inhibited IL-13 expression in the skin of fibrotic mice [16], and therefore we hypothesize that EHP-101 (oral VCE-004.8) could also affect the expression of profibrotic cytokines such as IL-13 that could explain the reduction of TNC expression.

SSc is a multi-factorial connective tissue disorder characterized by vascular injury, and by fibrosis of the skin and various internal organs. For instance, SSc patients typically show a reduction in the number of microvessels [50], and BLM challenge in mice is also associated to a reduction in the number and the perimeter of the vessels in the dermis. EHP-101 was able to recover the vascular morphology in BLM-mice

measured by CD31 expression. By inducing HIF-1α stabilization in endothelial cells, EHP-101 could upregulate the expression of VEGF [21], which is known to increase blood vessel length and area *in vivo* and *in vitro* [51–53]. On the other hand, there is considerable evidence that vascular damage is initiated by endothelial cell injury and activation [54]. The injured/activated endothelial cells may detach from the vascular endothelium, and the activation of endothelial cells also induces the expression of cell adhesion molecules, such as VCAM1 [55,56], which expression is reduced by EHP-101 treatment.

The RNA-Seq analysis from mice skin biopsies revealed that oral EHP-101 had a direct effect in the skin transcriptome by inhibiting the expression of several genes associated with the disease. In this sense, EHP-101 normalized the expression of a large number of genes associated to the inflammatory response and with the epithelial-mesenchymal transition process, which is mainly regulated by TGF-β [57]. For instance, genes downregulated by EHP-101 in BLM mice includes matrix metalloproteinase-3 (Mmp3), cytochrome b-245 heavy chain (Cybb), lymphocyte antigen 6E (Ly6e), Vcam1 and the Integrin alpha-5 (Itga5), which are part of a TGF-β responsive transcriptomic signature previously identified in BLM-induced skin fibrosis [58]. Furthermore, the expression of Type VII collagen (Col7a1) is also directly related to TGF-β signaling in the skin of human SSc patients [59] and its expression level was also significantly reduced by EHP-101 treatment. We additionally found that EHP-101 reduced the expression of the C-C motif chemokine 2 (Ccl2) and the interleukin 13 receptor subunit alpha 1 (Il13ra1), two processes regulated by the TGF-β/PPARγ signaling pathway [11]. These have been studied as biomarkers and possible targets for the management and treatment of SSc in humans [60,61]. Given the relevance of the TGF-β signaling in this disease [62], our results provide additional evidence that EHP-101 can alleviate skin inflammation, vascular damage and fibrosis associated to SSc, also showing that oral administration is feasible.

Acknowledgements

This work was partially supported by grants SAF2014-53763-P and SAF2017-87701-R to EM from the Ministry of the Economy and Competition (MINECO) co-financed with the European Union FEDER funds. VivaCell Biotechnology España also supported this work and had no further role in study design, the collection, analysis and interpretation of data, in the writing of the report, or in the decision to submit the paper for publication.

Conflict of interest

The authors state no conflict of interest.

References

[1] A. Leask, Toward personalized medicine in scleroderma: classification of scleroderma patients into stable “inflammatory” and “fibrotic” subgroups, J. Invest. Dermatol. 132 (5) (2012) 1329–1331.
[2] T.R. Katsumoto, M.L. Whitfield, M.K. Connolly, The pathogenesis of systemic sclerosis, Annu. Rev. Pathol. 6 (2011) 509–537.
[3] A. Milano, S.A. Pendergrass, J.L. Sargent, L.K. George, T.H. McCalmont, M.K. Connolly, et al., Molecular subsets in the gene expression signatures of scleroderma skin, PLoS One 3 (7) (2008) e2696.
[4] N. Barrie, N. Manolios, The endocannabinoid system in pain and inflammation: its relevance to rheumatic disease, Eur. J. Rheumatol. 4 (3) (2017) 210–218.
[5] M. Pistis, S.E. O'Sullivan, The role of nuclear hormone receptors in cannabinoid function, Adv. Pharmacol. 80 (2017) 291–328.
[6] E. Garcia-Gonzalez, E. Selvi, E. Balistreri, S. Lorenzini, R. Maggio, M.R. Natale, et al., Cannabinoids inhibit fibrogenesis in diffuse systemic sclerosis fibroblasts, Rheumatology (Oxford) 48 (9) (2009) 1050–1056.
[7] S. Marquart, P. Zerr, A. Akhmetshina, K. Palumbo, N. Reich, M. Tomcik, et al., Inactivation of the cannabinoid receptor CB1 prevents leukocyte infiltration and experimental fibrosis, Arthritis Rheum. 62 (11) (2010) 3467–3476.
[8] A. Akhmetshina, C. Dees, N. Busch, J. Beer, K. Sarter, J. Zwerina, et al., The cannabinoid receptor CB2 exerts antifibrotic effects in experimental dermal fibrosis, Arthritis Rheum. 60 (4) (2009) 1129–1136.
[9] A. Servettaz, N. Kavian, C. Nicco, V. Deveaux, C. Chereau, A. Wang, et al., Targeting the cannabinoid pathway limits the development of fibrosis and autoimmunity in a mouse model of systemic sclerosis, Am. J. Pathol. 177 (1) (2010) 187–196.
[10] R.B. Clark, The role of PPARs in inflammation and immunity, J. Leukoc. Biol. 71 (3) (2002) 388–400.
[11] A.T. Dantas, M.C. Pereira, M.J. de Melo Rego, L.F. da Rocha Jr., R. Pitta Ida, C.D. Marques, et al., The role of PPAR gamma in systemic sclerosis, PPAR Res. 2015 (2015) 124624.
[12] A. Galli, D.W. Crabb, E. Ceni, R. Salzano, T. Mello, G. Svegliati-Baroni, et al., Antidiabetic thiazolidinediones inhibit collagen synthesis and hepatic stellate cell activation in vivo and in vitro, Gastroenterology 122 (7) (2002) 1924–1940.
[13] K.H. Bae, J.B. Seo, Y.A. Jung, H.Y. Seo, S.H. Kang, H.J. Jeon, et al., Lobeglitazone, a novel peroxisome proliferator-activated receptor gamma agonist, attenuates renal fibrosis caused by unilateral ureteral obstruction in mice, Endocrinol. Metab. (Seoul) 32 (1) (2017) 115–123.
[14] J.E. Milam, V.G. Keshamouni, S.H. Phan, B. Hu, S.R. Gangireddy, C.M. Hogaboam, et al., PPAR-gamma agonists inhibit profibrotic phenotypes in human lung fibroblasts and bleomycin-induced pulmonary fibrosis, Am. J. Physiol. Lung Cell. Mol. Physiol. 294 (5) (2008) L891–L901.
[15] E.G. Gonzalez, E. Selvi, E. Balistreri, A. Akhmetshina, K. Palumbo, S. Lorenzini, et al., Synthetic cannabinoid ajulemic acid exerts potent antifibrotic effects in experimental models of systemic sclerosis, Ann. Rheum. Dis. 71 (9) (2012) 1545–1551.
[16] C. del Río, C. Navarrete, J.A. Collado, M.L. Bellido, M. Gómez-Cañas, M.R. Pazos, et al., The cannabinoid quinol VCE-004.8 alleviates bleomycin-induced scleroderma and exerts potent antifibrotic effects through peroxisome proliferator-activated receptor-γ and CB2 pathways, Sci. Rep. 6 (2016) 21703.
[17] J. Wei, H. Zhu, K. Komura, G. Lord, M. Tomcik, W. Wang, et al., A synthetic PPAR-gamma agonist triterpenoid ameliorates experimental fibrosis: PPAR-gamma-independent suppression of fibrotic responses, Ann. Rheum. Dis. 73 (2) (2014) 446–454.
[18] N. Ruzehaji, C. Frantz, M. Ponsoye, J. Avouac, S. Pezet, T. Guilbert, et al., Pan PPAR agonist IVA337 is effective in prevention and treatment of experimental skin fibrosis, Ann. Rheum. Dis. 75 (12) (2016) 2175–2183.
[19] E. Balistreri, E. Garcia-Gonzalez, E. Selvi, A. Akhmetshina, K. Palumbo, S. Lorenzini, et al., The cannabinoid WIN55, 212–2 abrogates dermal fibrosis in scleroderma bleomycin model, Ann. Rheum. Dis. 70 (4) (2011) 695–699.
[20] M.P. Motwani, F. Bennett, P.C. Norris, A.A. Maini, M.J. George, J. Newson, et al., Potent anti-inflammatory and pro-resolving effects of anabasum in a human model of self-resolving acute inflammation, Clin. Pharmacol. Ther. (2017).
[21] C. Navarrete, F. Carrillo-Salinas, B. Palomares, M. Mecha, C. Jimenez-Jimenez, L. Mestre, et al., Hypoxia mimetic activity of VCE-004.8, a cannabidiol quinone derivative: implications for multiple sclerosis therapy, J. Neuroinflam. 15 (1) (2018) 64.
[22] T. Ashcroft, J.M. Simpson, V. Timbrell, Simple method of estimating severity of pulmonary fibrosis on a numerical scale, J. Clin. Pathol. 41 (4) (1988) 467–470.
[23] R.H. Hubner, W. Gitter, N.E. El Mokhtari, M. Mathiak, M. Both, H. Bolte, et al., Standardized quantification of pulmonary fibrosis in histological samples, Biotechniques 44 (4) (2008) pp. 507–11, 14–7.
[24] A.M. Bolger, M. Lohse, B. Usadel, Trimmomatic: a flexible trimmer for Illumina sequence data, Bioinformatics 30 (15) (2014) 2114–2120.
[25] D. Kim, B. Langmead, S.L. Salzberg, HISAT: a fast spliced aligner with low memory requirements, Nat. Meth. 12 (4) (2015) 357–360.
[26] Y. Liao, G.K. Smyth, W. Shi, featureCounts: an efficient general purpose program for assigning sequence reads to genomic features, Bioinformatics 30 (7) (2014) 923–930.
[27] M.I. Love, W. Huber, S. Anders, Moderated estimation of fold change and dispersion for RNA-seq data with DESeq2, Genome Biol. 15 (12) (2014) 550.
[28] G. Yu, L.G. Wang, Y. Han, Q.Y. He, clusterProfiler: an R package for comparing biological themes among gene clusters, OMICS 16 (5) (2012) 284–287.
[29] A. Liberzon, C. Birger, H. Thorvaldsdottir, M. Ghandi, J.P. Mesirov, P. Tamayo, The Molecular Signatures Database (MSigDB) hallmark gene set collection, Cell Syst. 1 (6) (2015) 417–425.
[30] T. Yamamoto, S. Takagawa, I. Katayama, K. Yamazaki, Y. Hamazaki, H. Shinkai, et al., Animal model of sclerotic skin. I: local injections of bleomycin induce sclerotic skin mimicking scleroderma, J. Invest. Dermatol. 112 (4) (1999) 456–462.
[31] T. Yamamoto, I. Katayama, Vascular changes in bleomycin-induced scleroderma, Int. J. Rheumatol. 2011 (2011) 270938.
[32] T.A. Wynn, Cellular and molecular mechanisms of fibrosis, J. Pathol. 214 (2) (2008) 199–210.
[33] T. Yamamoto, Y. Takahashi, S. Takagawa, I. Katayama, K. Nishioka, Animal model of sclerotic skin. II. Bleomycin induced scleroderma in genetically mast cell deficient WBB6F1-W/W(V) mice, J. Rheumatol. 26 (12) (1999) 2628–2634.
[34] J. Varga, D. Abraham, Systemic sclerosis: a prototypic multisystem fibrotic disorder, J. Clin. Invest. 117 (3) (2007) 557–567.
[35] M. Matucci-Cerinic, B. Kahaleh, F.M. Wigley, Review: evidence that systemic sclerosis is a vascular disease, Arthritis Rheum. 65 (8) (2013) 1953–1962.
[36] V. Liakouli, P. Cipriani, P. Di Benedetto, P. Ruscitti, F. Carubbi, O. Berardicurti, et al., The role of extracellular matrix components in angiogenesis and fibrosis: possible implication for Systemic Sclerosis, Mod. Rheumatol. 1–11 (2018).
[37] D. Ummarino, Systemic sclerosis: tenascin C perpetuates tissue fibrosis, Nat. Rev. Rheumatol. 12 (7) (2016) 375.
[38] J.E. Pope, Connective tissue disease: reflections on the EULAR recommendations for the treatment of systemic sclerosis, Nat. Rev. Rheumatol. 13 (3) (2017) 134–136.
[39] A.K. Ghosh, S. Bhattacharyya, J. Wei, S. Kim, Y. Barak, Y. Mori, et al., Peroxisome proliferator-activated receptor-gamma abrogates Smad-dependent collagen stimulation by targeting the p300 transcriptional coactivator, FASEB J. 23 (9) (2009)

2968–2977.
[40] L. Mestre, F. Docagne, F. Correa, F. Loria, M. Hernangomez, J. Borrell, et al., A cannabinoid agonist interferes with the progression of a chronic model of multiple sclerosis by downregulating adhesion molecules, Mol. Cell. Neurosci. 40 (2) (2009) 258–266.
[41] S.M. Jackson, F. Parhami, X.P. Xi, J.A. Berliner, W.A. Hsueh, R.E. Law, et al., Peroxisome proliferator-activated receptor activators target human endothelial cells to inhibit leukocyte-endothelial cell interaction, Arterioscler. Thromb. Vasc. Biol. 19 (9) (1999) 2094–2104.
[42] V. Pasceri, H.D. Wu, J.T. Willerson, E.T. Yeh, Modulation of vascular inflammation in vitro and in vivo by peroxisome proliferator-activated receptor-gamma activators, Circulation 101 (3) (2000) 235–238.
[43] T. Collins, M.A. Read, A.S. Neish, M.Z. Whitley, D. Thanos, T. Maniatis, Transcriptional regulation of endothelial cell adhesion molecules: NF-kappa B and cytokine-inducible enhancers, FASEB J. 9 (10) (1995) 899–909.
[44] J. Munoz-Luque, J. Ros, G. Fernandez-Varo, S. Tugues, M. Morales-Ruiz, C.E. Alvarez, et al., Regression of fibrosis after chronic stimulation of cannabinoid CB2 receptor in cirrhotic rats, J. Pharmacol. Exp. Ther. 324 (2) (2008) 475–483.
[45] K. Midwood, S. Sacre, A.M. Piccinini, J. Inglis, A. Trebaul, E. Chan, et al., Tenascin-C is an endogenous activator of Toll-like receptor 4 that is essential for maintaining inflammation in arthritic joint disease, Nat. Med. 15 (7) (2009) 774–780.
[46] Y. Ji, J. Liu, Z. Wang, N. Liu, W. Gou, PPARgamma agonist, rosiglitazone, regulates angiotensin II-induced vascular inflammation through the TLR4-dependent signaling pathway, Lab. Invest. 89 (8) (2009) 887–902.
[47] W. Wahli, L. Michalik, PPARs at the crossroads of lipid signaling and inflammation, Trends Endocrinol. Metab. 23 (7) (2012) 351–363.
[48] H.A. Makhluf, J. Stepniakowska, S. Hoffman, E. Smith, E.C. LeRoy, M. Trojanowska, IL-4 upregulates tenascin synthesis in scleroderma and healthy skin fibroblasts, J. Invest. Dermatol. 107 (6) (1996) 856–859.
[49] M. Jinnin, H. Ihn, Y. Asano, K. Yamane, M. Trojanowska, K. Tamaki, Upregulation of tenascin-C expression by IL-13 in human dermal fibroblasts via the phosphoinositide 3-kinase/Akt and the protein kinase C signaling pathways, J. Invest. Dermatol. 126 (3) (2006) 551–560.
[50] M. Manetti, S. Guiducci, M. Ruffo, I. Rosa, M.S. Faussone-Pellegrini, M. Matucci-Cerinic, et al., Evidence for progressive reduction and loss of telocytes in the dermal cellular network of systemic sclerosis, J. Cell Mol. Med. 17 (4) (2013) 482–496.
[51] P.U. Magnusson, C. Looman, A. Ahgren, Y. Wu, L. Claesson-Welsh, R.L. Heuchel, Platelet-derived growth factor receptor-beta constitutive activity promotes angiogenesis in vivo and in vitro, Arterioscler. Thromb. Vasc. Biol. 27 (10) (2007) 2142–2149.
[52] M.N. Nakatsu, R.C. Sainson, S. Perez-del-Pulgar, J.N. Aoto, M. Aitkenhead, K.L. Taylor, et al., VEGF(121) and VEGF(165) regulate blood vessel diameter through vascular endothelial growth factor receptor 2 in an in vitro angiogenesis model, Lab. Invest. 83 (12) (2003) 1873–1885.
[53] D.I. Holmes, I. Zachary, The vascular endothelial growth factor (VEGF) family: angiogenic factors in health and disease, Genome Biol. 6 (2) (2005) 209.
[54] D. Abraham, O. Distler, How does endothelial cell injury start? The role of endothelin in systemic sclerosis, Arthritis Res. Ther. 9 (Suppl 2) (2007) S2.
[55] A.E. Koch, L.B. Kronfeld-Harrington, Z. Szekanecz, M.M. Cho, G.K. Haines, L.A. Harlow, In,, et al., situ expression of cytokines and cellular adhesion molecules in the skin of patients with systemic sclerosis. Their role in early and late disease, Pathobiology 61 (5–6) (1993) 239–246.
[56] B.J. Rabquer, Y. Hou, F. Del Galdo, G. Kenneth Haines 3rd., M.L. Gerber, S.A. Jimenez, et al., The proadhesive phenotype of systemic sclerosis skin promotes myeloid cell adhesion via ICAM-1 and VCAM-1, Rheumatology (Oxford) 48 (7) (2009) 734–740.
[57] J. Xu, S. Lamouille, R. Derynck, TGF-beta-induced epithelial to mesenchymal transition, Cell Res. 19 (2) (2009) 156–172.
[58] J.L. Sargent, Z. Li, A.O. Aliprantis, M. Greenblatt, R. Lemaire, M.H. Wu, et al., Identification of optimal mouse models of systemic sclerosis by interspecies comparative genomics, Arthritis Rheumatol. 68 (8) (2016) 2003–2015.
[59] L. Rudnicka, J. Varga, A.M. Christiano, R.V. Iozzo, S.A. Jimenez, J. Uitto, Elevated expression of type VII collagen in the skin of patients with systemic sclerosis. Regulation by transforming growth factor-beta, J. Clin. Invest. 93 (4) (1994) 1709–1715.
[60] M.B. Greenblatt, J.L. Sargent, G. Farina, K. Tsang, R. Lafyatis, L.H. Glimcher, et al., Interspecies comparison of human and murine scleroderma reveals IL-13 and CCL2 as disease subset-specific targets, Am. J. Pathol. 180 (3) (2012) 1080–1094.
[61] L.M. Rice, C.M. Padilla, S.R. McLaughlin, A. Mathes, J. Ziemek, S. Goummih, et al., Fresolimumab treatment decreases biomarkers and improves clinical symptoms in systemic sclerosis patients, J. Clin. Invest. 125 (7) (2015) 2795–2807.
[62] J. Varga, B. Pasche, Transforming growth factor beta as a therapeutic target in systemic sclerosis, Nat. Rev. Rheumatol. 5 (4) (2009) 200–206.